REVIEW ARTICLE

Recent advances in nanorobotic manipulation inside scanning electron microscopes

Chaoyang Shi[1], Devin K Luu[1], Qinmin Yang[2], Jun Liu[1], Jun Chen[1], Changhai Ru[3], Shaorong Xie[4], Jun Luo[4], Ji Ge[1] and Yu Sun[1]

A scanning electron microscope (SEM) provides real-time imaging with nanometer resolution and a large scanning area, which enables the development and integration of robotic nanomanipulation systems inside a vacuum chamber to realize simultaneous imaging and direct interactions with nanoscaled samples. Emerging techniques for nanorobotic manipulation during SEM imaging enable the characterization of nanomaterials and nanostructures and the prototyping/assembly of nanodevices. This paper presents a comprehensive survey of recent advances in nanorobotic manipulation, including the development of nanomanipulation platforms, tools, changeable toolboxes, sensing units, control strategies, electron beam-induced deposition approaches, automation techniques, and nanomanipulation-enabled applications and discoveries. The limitations of the existing technologies and prospects for new technologies are also discussed.

INTRODUCTION

A variety of nanomaterials, such as nanotubes, nanowires, plasmonic and semiconductive nanomaterials, and two-dimensional materials, such as graphene and transition metal dichalcogenides, require their properties to be characterized to understand their behaviors and explore their applications in nanoelectronics, nanophotonics, biology, and medicine[1–5]. The fabrication and development of nanoscaled devices and nanoelectromechanical systems (NEMS) that use these nanomaterials also require precise techniques for positioning, sensing, and assembly with nanometer resolutions[3,6,7].

Techniques for constructing nanoscaled devices can be categorized into top–down, bottom–up, and nanomanipulation-enabled techniques[3,7]. The top–down approaches typically employ techniques such as X-ray electron beam lithography and nanoimprint lithography[8–10]. Bottom–up techniques, such as self-assembly, chemical synthesis or super-molecule techniques[11,12], are driven by the tendency of physical systems to minimize their potential energy. These techniques enable the construction of structures and devices via the direct assembly of atoms and molecules; however, modifying specific locations to adjust the device properties can be challenging. Nanorobotic manipulation is a complementary technique that enables flexible maneuvering and precise positioning of nanostructures for nano device assembly; it is particularly suitable for device prototyping and property tuning[3,13]. Papers that primarily focused on nanomanipulation applications and nanomanipulation inside an SEM were published in 2008, 2005, and previous years[8,13]. Conversely, this paper discusses technological advances and recent discoveries enabled by SEM-based nanomanipulation in addition to state-of-the-art applications.

The first nanorobotic manipulation experiment was performed by Eigler and Schweizer in 1990 (Ref. 14) with a scanning tunneling microscope (STM) to form the IBM logo by separately positioning 35 individual xenon atoms on a nickel substrate at low temperatures, which demonstrates atomic-level manipulation and fabrication. However, an STM requires the use of conductive probes and samples owing to its working principle[7]. To manipulate different types of materials, an atomic force microscope (AFM), which is a type of scanning probe microscope (SPM), is capable of subnanometer imaging and manipulation[15–17]. AFMs permit the manipulation of nanoscaled materials in ambient, aqueous, and vacuum environments, which render the technique capable of handling conductive, nonconductive, and biological materials[2,18]. However, performing simultaneous manipulation and imaging using AFMs remains challenging[13,17,19] because the acquisition of one frame of an image by raster scanning requires at least several minutes. In addition, the look-then-move control scheme and small scanning area and workspace limit its manipulation throughput[7,17].

A transmission electron microscope (TEM), which emits high-energy electrons that pass through a sample, is capable of subnanometer imaging. With the development of aberration correctors, state-of-the-art TEMs can achieve an imaging resolution of tens of picometers[20,21] and perform atomic-level measurements for structural dynamics. However, the working principle of TEMs demands special sample preparation, and the small specimen chamber and workspace of a TEM limit the capabilities of complex nanomanipulation[13]. Conversely, the SEM detects secondary electrons that are emitted by the sample surface when struck by an electron beam, which provides real-time nanometer-level imaging[7]. Compared with TEMs, SEMs have

[1]Department of Mechanical and Industrial Engineering, University of Toronto, Toronto, ON, Canada M5S 3G8; [2]Department of Control Science and Engineering, Zhejiang University, Hangzhou 310058, China; [3]Robotics and Microsystems Center, Soochow University, Suzhou 215021, China and [4]School of Mechatronic Engineering and Automation, Shanghai University, Shanghai 200072, China
Correspondence: Ji Ge (jige@mie.utoronto.ca) or Yu Sun (sun@mie.utoronto.ca)
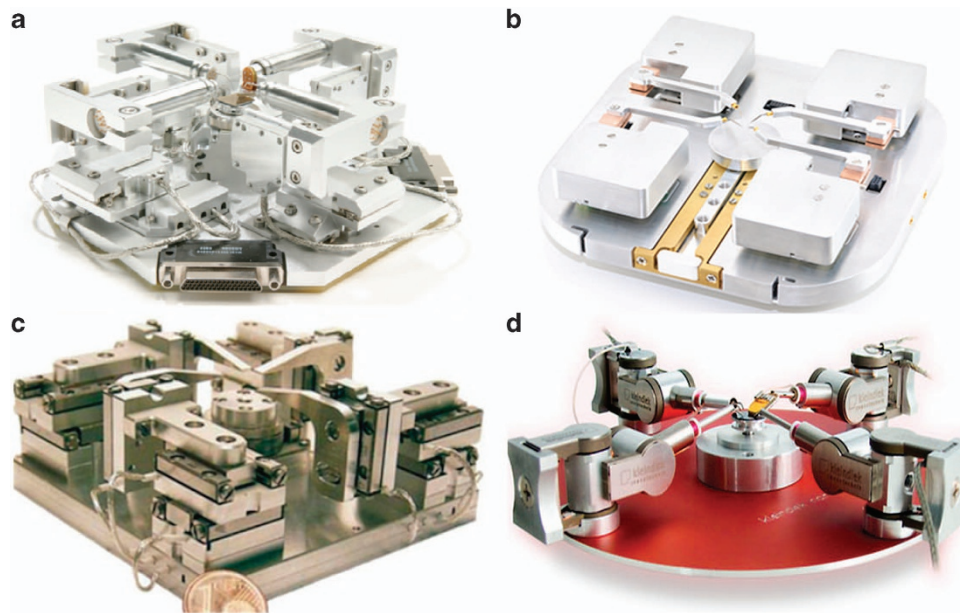Received: 23 February 2016; revised: 2 April 2016; accepted: 5 April 2016

Figure 1 Examples of commercial nanomanipulation systems. (**a**) Zyvex. (**b**) Lifeforce. (**c**) SmarAct system. (**d**) Kleindiek.

substantially larger specimen chambers and scanning areas, which enable the integration of complex nanomanipulation systems. These advantages enable simultaneous imaging and precise nanomanipulation[3].

A number of nanorobotic manipulation systems have been constructed for operation inside an SEM since the 1990s[8,13,22]. Hatamura and Tomomasa pioneered the development of a nanomanipulation system inside an SEM[23–25]. The system consisted of two manipulators, a controllable base, a customized force sensor, joy sticks, and an optical microscope, which enabled haptic and position control. Automated pick-and-place of 30 μm spheres inside an SEM was demonstrated[24]. The system was only capable of manipulating relatively large micrometer-sized objects and was not capable of performing complex assembly tasks owing to the mechanical wobbling of the manipulators and relatively large end-effectors.

Recently, nanorobotic manipulation platforms with multiple degrees of freedom (DOFs) and piezoelectric actuators have been constructed inside SEMs for manipulating nanoscaled objects with nanometer resolution, which enables the realization of complicated tasks that range from mechanical tensile testing and electrical probing of nanomaterials[26–30], electronic and photonic device prototyping[1,22,31], NEMS assembly[31–34], biological cell characterization and manipulation[3,35,36] and subcellular organelle extraction[35,37]. State-of-the-art SEM-based nanomanipulation systems are also integrated with AFMs and focused ion beam (FIB) systems, as well as various tools[38] and exchangeable toolboxes[39]. With these advances, powerful nano-laboratories have been established that are capable of simultaneous imaging, fabrication, and nanomanipulation[40–43] with high efficiency and reproducibility via the use of emerging automation techniques[30,44–46].

NANOMANIPULATION SYSTEMS INSIDE SEMS

Nanomanipulation systems inside SEMs primarily consist of an actuation unit, a sensing unit, control strategies, and nanotools. Techniques such as electron-beam-induced deposition (EBID) are often employed for nanoscaled welding and assembly. This section summarizes recent advances in these technologies.

Actuation

Actuators that are employed for nanomanipulation inside an SEM must be compact, vacuum-compatible, and capable of generating accurate motions without interfering with electron microscopy imaging. Thermal actuators cannot effectively dissipate heat in a vacuum environment, whereas electric motors and voice coil actuators generate magnetic fields that can interfere with electron optics. Piezoelectric actuators that are governed by the inverse piezoelectric effect overcome these challenges[47,48] and are capable of generating large forces in the kilo-Newton range with subnanometer positioning resolution and a high bandwidth[49]. A number of piezoelectric actuator-based nanomanipulators with multiple DOFs have been developed for precise positioning and manipulation of micro- and nanoscaled objects by companies (for example, Zyvex, Kleindiek, SmarAct, Toronto Nanoinstrumentation, and Attocube) and academia[33,41,42,50–54].

The most common configuration of actuators for nanomanipulation is a coarse and fine positioner combination or a single actuator for both coarse and fine positioning. For instance, Zyvex and Lifeforce systems consist of four quadrants of three-DOF nanomanipulators, each of which uses two separate three-axis piezoelectric actuator units for coarse positioning and fine positioning, respectively, as shown in Figures 1a and b. The coarse positioners move according to the slip-stick actuation principle[49,55] to generate stepwise motions at a high speed and with total motion ranges on the order of centimeters but with a low resolution and accuracy owing to unrepeatable steps. The separate fine unit uses piezo stacks, piezo tubes or flexure-guided mechanisms[47,55] to precisely position the end-effector and enables a large fine motion range on the order of tens of micrometers (refer to Table 1). Kleindiek and SmarAct systems are composed of four quadrants of three-DOF nanomanipulators, each of which only uses one three-axis piezoelectric actuator unit. The single piezoelectric element either operates as a coarse actuator in the slip-stick mode or operates as a fine actuator solely in stick mode. This configuration produces a compact design but can induce undesired vibration during dynamic positioning, and the fine motion range is typically limited to < 2 μm.

Table 1 Summary of commercial nanomanipulation systems

System	Speed	Coarse motion range	Fine motion range	DOF	Coarse resolution	Fine resolution
Zyvex S100	3 mm s^{-1}	12 mm XYZ	50 µm for XY; 10 µm for Z;	Four units with 24 axes	100-nm open loop	5-nm open loop
Xidex NanoBot NX-2000	1 mm s^{-1}	12 mm XYZ	5 µm XYZ	Two units with six axes	50-nm open loop	1-nm open loop
Oxford Instruments OmniProbe 400	N/A	4 mm XYZ	Not specified	One unit (four axes with one rotation)	10-nm closed loop	N/A
TNI LifeForce	> 10 mm s^{-1}	10 mm XY 5 mm Z	30 µm XYZ	Four units with 12 axes	< 100-nm open loop	0.1-nm open loop 1-nm closed loop
Kleindiek MM3A	2 mm s^{-1} telescoping; 10 mm s^{-1} rotation	12-mm telescoping; 240° rotation	Not specified	One translation Two rotations	5-nm open loop rotation; 0.5-nm open loop translation	N/A
SmarAct SLC	> 10 mm s^{-1}	10 mm XYZ	1.5 µm XYZ	Four units with 12 axes	20-nm closed loop	1-nm closed loop
Imina miBot BT-11	2.5 mm s^{-1}	Unlimited XY 10 mm Z	440 nm XY 780 nm Z	Two translations Two rotations	40-nm open loop	0.5-nm open loop

Abbreviation: DOF, degrees of freedom.

In addition to these stationary platforms, mobile nanomanipulators have also been developed[56–59]. Their actuation is typically based on the slip-stick principle[60] or the inchworm mobile mechanism[59] using piezoceramic actuators. These mobile platforms perform manipulation with nanometer accuracy. They collaborate among multiple robots and are capable of moving longer distances. However, the precise tracking of the position and orientation of the mobile robots is challenging. Conversely, stationary nanomanipulation platforms can generate more precise and accurate motion, are easier to control without localization and coordination difficulties, and facilitate automated nanomanipulation.

Sensing
An important consideration for sensing in the vacuum environment is that heat generated from powering sensors cannot be effectively dissipated, which can cause instability owing to thermal drift. This section discusses advances in position, depth, and force sensing that are employed in SEM-based nanomanipulation.

Position sensing. Piezoelectric actuators inherently exhibit nonlinear characteristics of hysteresis and creep[49], which degrade positioning precision and can cause system instability[61]. Three types of position sensors exist for integration with piezoelectric actuators, including capacitive, optical encoder-based and strain gauge-based sensors. Although piezoelectric actuators inherently possess sensing capabilities for estimating force and/or displacement[62], piezoelectric self-sensing is difficult to implement in piezoelectric stacks, which is typically employed for the construction of nanopositioners.

Capacitive sensors provide a noncontact, low-power and direct position measurement approach for obtaining accurate nanometer and subnanometer measurements with a bandwidth up to 10 kHz and minimum heating[63]. However, capacitive sensors are costly and difficult for accurate assembly[64] and are limited to short-range measurements within a couple of millimeters[65]. Optical encoder-based sensors generate incremental measurement readings that are capable of providing accurate position feedback for large-motion ranges (for example, tens of millimeters) at nanometer resolutions[41]. However, optical elements generate heat, which can cause thermal drift in surrounding components inside the vacuum chamber of an SEM[64]. Similarly, strain gauge-based sensors also suffer from thermal drift problems. When strain gauge-based sensors are utilized for position sensing inside an SEM, measuring the charging and discharging time of a capacitor that is connected to a strain gauge via time-to-digital conversion has been proven to generate 50 times less heat than optical encoders while achieving nanometer resolutions[64].

Depth sensing. Height control in nanomanipulation is challenging owing to the lack of depth information[66–68]. Depth sensing can be achieved using a force sensor to touch a target[69]. Piezoresistive AFM cantilevers have been applied for height estimation[70]. A vibrating piezoelectric bimorph actuator[71], in which the vibration amplitude decreases upon contact with a substrate or target, was also demonstrated. Because force sensors are difficult to integrate with nanomanipulation tools, an image-processing-based approach was developed[72]. In this approach, after the nanomanipulator tool contacts the target substrate, lowering of the tool causes horizontal sliding, which is detected by image processing. After the relative vertical position of the nanomanipulation tool relative to the target substrate is detected, closed-loop position control along the Z-direction can be conducted for depth control.

Vision-based depth sensing was also realized by installing an optical microscope and camera to the SEM chamber wall for detecting tool tip depth[73,74]. This method's detection resolution is limited by the Abbe diffraction limit of optical microscopy (that is, hundreds of nanometers). Stereo imaging was employed to determine tool depth by tilting either the SEM sample stage[75,76] or the electron beam[67]. Mechanical components in stereo methods must be manufactured with tight tolerances, and image drift compensation must be carefully performed to achieve accurate depth sensing.

Force sensing. Force sensors provide force feedback in nanomanipulation[77,78]. Microelectromechanical systems (MEMs) capacitive force sensors utilize comb structures to detect capacitance changes that are induced by externally applied forces[79,80]. A

Table 2 MEMS grippers that are used in nanomanipulation

Principle	Actuation structure	Fabrication	Actuation voltage	Motion range	Usage in nanomanipulation
Electrostatic driven	Comb drive	DRIE of SOI[101,102]	Medium voltage	~ 10 μm	Pick-and-place of nano spheres and micro particles[106–108]
Electrothermal driven	U-shaped and V-shaped beams	RIE of SOI[103]	Low voltage	~2 μm	Pick-and-place of nanowires[109,110]; assembly to form customized scanning probe tips[111,112]
Piezoelectric driven	Bimorph	Ultrasonic machining of piezoceramic plates[104,105]	High voltage	> 20 μm	Manipulation of CNTs, micro grains and copper spheres[105,113–115]

Abbreviation: DRIE, deep reactive ion etching; SOI, silicon on insulator.
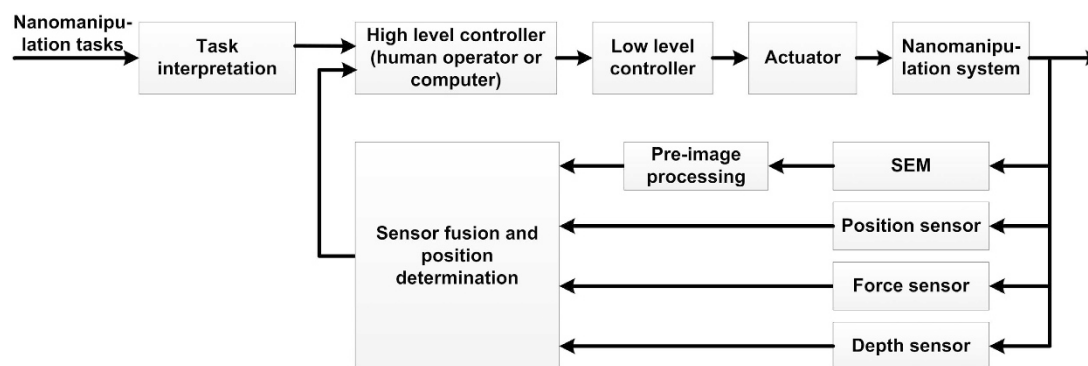

Figure 2 Control architecture of nanorobotic manipulation inside an SEM; scanning electron microscope.

two-axis MEMS capacitive force sensor[81,82] and an improved six-axis capacitive force sensor[83] were constructed via deep reactive ion etching of silicon on insulator (SOI) substrates. These capacitive force sensors are capable of measuring forces from a few nanonewtons to micronewtons.

MEMS piezoresistive force sensors, which are formed by ion implantation, have also been developed for nanoscaled applications[77,79]. Piezoresistive force sensors were mounted on a nanomanipulator to provide high-accuracy force measurements that range from nanonewtons to millinewtons[84]. By using piezoresistive force sensors, mechanical indentation for stiffness determination of 2D materials and scanning for surface topography were achieved[45].

When AFM probes are used for force sensing, an applied force can be determined from Hooke's law[85,86]. The stiffness of an AFM probe can be calibrated using a reference cantilever of a known stiffness[87]. Image processing can be conducted to measure AFM probe deflections and determine the applied force. In[88], vision-based force sensing was achieved using a deformable template-matching algorithm to visually determine the force distribution acts on a linearly elastic object using the contour information in an image. The effectiveness was validated using both AFM probes and microgrippers.

Nanotools and tool exchangers

A number of nanotools are employed as end-effectors to perform nanomanipulation tasks, such as AFM probes, tungsten needles, and MEMS grippers. AFM probes and tungsten needles are the most popular end-effectors for nanomanipulation owing to their versatility and commercial availability. A nanomanipulator that is equipped with an AFM probe can perform topography imaging,

indentation, stretching, cutting and pushing, pick-and-place operation and assembly, and nanolithography[2,8,40,70]. The AFM cantilever structure can be modified by FIB etching and deposition to create various types of application-specific tools. For instance, AFM probes were modified to have a flat tip[86,89], stiff needle tip[87,90–93], knife blade tip[94] and fork tips[95,96] for cellular and intracellular characterization and cell manipulation. Tungsten probes are fabricated and sharpened by electrochemical etching to obtain a high-aspect ratio. They were employed to perform tensile tests for mechanical characterization[97] and pick-and-place assembly[98], as well as electrical characterization of nanoscaled semiconductor devices and nanomaterials[26,30,99].

Compared with these single-ended tools, MEMS grippers can be precisely actuated with large forces to effectively overcome material-substrate adhesion and perform reliable grasping of nano objects[100]. MEMS grippers are typically driven by electrostatic, electrothermal, and piezoelectric actuators[47,77]. They are made with feature structures using different fabrication methods[101–105], and have been applied for various nanomanipulation tasks[106–112], as summarized in Table 2. Although electrostatic actuation has low power, it requires relatively high actuation voltages. Electrothermal microgrippers operate under low voltages, produce short travel ranges, and can induce thermal drift to surrounding materials. The piezoelectrically driven microgrippers that are reported in Refs. 105,113–115 utilized piezoelectric bimorph structures and produced a motion range greater than 20 μm at high actuation voltages. Sensors can also be constructed in microgrippers for force-controlled grasping[116]. Tool exchangers have also been developed for easy replacement of broken tools and the modification of different types of end tools without opening the high-vacuum chamber of an SEM. A toolbox array with different tip morphologies, which are termed Nanobits, was fabricated by

electron beam lithography and silicon processing[39,117]. A micro-gripper detached these tools from the tool array and assembled them to AFM probes or other end-effectors to form scanning probe tips[112,117]. The commercially available Oxford Instruments OmniProbe 400 system also features an *in situ* tool exchange and probe tip sharpening for repairing or replacing broken tools.

Control

For nanomanipulation inside an SEM, a look-and-manipulation scheme can be implemented to accomplish closed-loop control, as depicted in Figure 2. A high-level controller is responsible for supervising tasks, such as target tracking, trajectory planning, error handling, and the parallel execution of subtasks. With multiple types of sensing modalities (for example, force sensing, depth sensing, and positioning sensing), a sensor fusion approach can be employed to enhance the success rate of nanomanipulation and provide a basis for high-level control, decision-making, planning and fault-tolerance handling. A low-level controller receives commands from a high-level controller to generate driving signals for nanopositioning/nanomanipulation.

The low-level controller can be implemented via feedback, feedforward, or feedback–feedforward control[61,118,119]. A feedforward controller determines control signals according to the knowledge and modes of hysteresis, creep, and vibration. Because feedforward control does not rely on sensor feedback for high-bandwidth nanopositioning, the advantages are low cost and low hardware complexity[119,120]. In addition, techniques such as input shaping can be utilized to mitigate vibration[121]. However, the accuracy of feedforward techniques is dependent on both the model and the parameters identified in the model, which can change over time, especially in dynamic scenarios and the vacuum environment inside an SEM[122]. Feedback control utilizes sensor feedback, relaxes modeling requirements, and achieves better performance in terms of accuracy, vibration suppression, and uncertainty/disturbance rejection[61]. However, feedback-controlled nanopositioning has low bandwidth and requires sensor integration in the hardware platform. Therefore, feedforward- and feedback-controlled nanopositioning were attempted for higher bandwidth and higher accuracy[30].

To achieve nanoscaled manipulation and assembly tasks, control approaches have been developed for tele-operated and automated nanomanipulation[49,123,124]. In tele-operated nanomanipulation, haptic and visual feedback are usually acquired and presented to a human operator. The operator sends task commands to the nanomanipulators via a joystick or a macro-manipulator. Virtual reality techniques have been introduced to enhance this human-in-the-loop control system by enabling the operator to feel immersed in the environment based on various sensory cues[125,126]. Teleoperation involves significant human intervention and requires significant operator skills. Tele-operated nanomanipulation is slow and exhibits poor repeatability.

For automated nanomanipulation, real-time SEM visual feedback is important for providing visual guidance and realizing closed-loop control. To circumvent challenges such as SEM image noise and drift, image denoising and drift compensation methods were implemented using graphics processing unit (GPU) techniques[26,127]. SEM tracking algorithms can be classified into feature-based methods, model-based methods and hybrid methods[88,128–132]. They are commonly employed to provide a nanomanipulation system with visual feedback for automated operation.

Electron-beam-induced deposition-assisted techniques

Electron-beam-induced deposition (EBID) is extensively applied inside SEMs as an important technique to deposit materials for welding and assembly at the nanoscale[42,133–135]. EBID involves the introduction of precursor gases into an SEM chamber from a nozzle after vaporization or sublimation. The gas molecules are subsequently irradiated by high-energy electrons, which decompose precursor molecules by secondary electrons that are diffracted from the irradiation spot and cause the deposition of nonvolatile fragments[136]. Several precursors are available for EBID to deposit various metals, dielectrics, and semiconductor materials, which render this technology a useful assistive technology for nanomanipulation, such as bonding end-effectors with materials[50,137] for pick-and-place operation, soldering different materials for characterization[137] and assembly[42,134], and sensor instrumentation[138–140]. EBID can also be employed to remove materials when oxygen gas is introduced as a precursor[141,142]. EBID and nanomanipulation were employed to produce high-purity and hybrid metallic nanowires[139,143], and various types of nanowires were grown with the introduction of different precursors. For instance, use of a nanomanipulator to precisely control the distance between a multi-walled CNT (MWCNT) field-emitter cathode and a tungsten probe emission anode, a high-purity platinum nanowire for intracellular PH sensing was formed using EBID with the introduction of trimethylcyclopentadienyl platinum ($CpPtMe_3$) as a precursor[139].

Hybrid system integration inside SEMs

The large chambers of SEMs enable other microscopy and manipulation instruments to be integrated and form a hybrid system. These hybrid systems include AFM/SEM, AFM/FIB/SEM, STM/SEM, AFM/ESEM, and SEM/TEM, which take advantage of the strength of each tool for performing characterization and nanomanipulation tasks. Table 3 summarizes and compares these hybrid systems.

SEM and AFM are complementary techniques for performing topography and morphology measurements[16,144,145]. The integration of an AFM inside an SEM enables simultaneous imaging and manipulation in real-time to perform SEM-guided topography analysis with high-resolution and force feedback. FIB has also been integrated for material etching and deposition. Several hybrid AFM/SEM and AFM/FIB/SEM systems have been developed[28,40,43,146,147], and commercial systems have also become available (for example, Semilab, Attocube, Trioptics, Nanonics Imaging Ltd, Kleindiek Nanotechnik).

Conventional AFM is based on laser beam deflection and is not typically integrated inside SEMs owing to space and optical path constraints. A commercial hybrid AFM/SEM system by DME-SPM Semilab was designed with modified laser paths inside an SEM, as shown in Figure 3a. Attocube Systems AG uses a fiber-optic configuration to construct an *in situ* AFM for operation inside an SEM (attoAFM/SEM) with a laser interferometer (Figure 3b). For these laser-based methods, laser alignment must be carefully performed, and low laser power must be maintained to mitigate thermal drift in the vacuum chamber of an SEM.

Conversely, laser-free AFM that uses self-sensing cantilevers and tuning forks can be readily integrated inside an SEM. The AFM/SEM system reported in Ref. 43 employed piezoresistive cantilevers to perform scanning and manipulation tasks with force feedback, as shown in Figure 3c. Dynamic AFMs that use a tuning fork with a QPlus or Akiyama probe were also integrated inside an SEM to scan samples that are especially susceptible to surface damage[148]. A dynamic AFM was integrated inside an SEM by Trioptics to realize surface topography with a large scanning area of 500 by 500 μm (Figure 3d). The 3TB4000 system from Nanonics Imaging Ltd. is an instrument that integrates an AFM, which is based on a tailor made Q-Plus tuning fork, an SEM and an FIB, as shown in Figure 3e. This hybrid instrument enables imaging with a large field of view from an SEM, three-dimensional (3D) material and end tool modifications with FIB, and high-resolution AFM imaging. Figure 3f shows another hybrid AFM/FIB/SEM system that uses

Table 3 Summary of hybrid systems

Hybrid systems	Configuration		End effectors	Functions	Limitations
AFM/SEM	Optics-based		AFM cantilevers	All available AFM modes (for example, DME-SPM Semilab, Attocube)	Thermal drift
	Optics-free	Contact mode	Piezoresistive cantilevers	Scanning and manipulation with force feedback[43]	Piezoresistive cantilevers only
		Dynamic mode	Tuning fork-based probes; Akiyama probe	Scanning for ultrasensitive surface topography[148]	No manipulation functions
AFM/FIB/SEM	Optics-free	Contact mode	Piezoresistive cantilevers	Fabrication, scanning and manipulation with force feedback[40]	Piezoresistive cantilevers only
		Dynamic mode	Tuning fork-based probes; Akiyama probe	Fabrication and surface topography (for example, Nanonics Imaging Ltd)	No manipulation functions
STM/SEM	Optics-free		Tungsten probes; Conductive AFM probes	Scanning with current feedback at both low and room temperatures[150,151]	Conductive probes only
AFM/ESEM	Optics-based		AFM cantilevers	All AFM modes available, especially for biological samples[52]	Thermal drift
SEM/TEM	TEM holder with piezo actuators		No limitations	Sample preparation in SEM, and manipulation in TEM[153]	Small workspace inside TEM

Abbreviations: AFM, atomic force microscope; SEM, scanning electron microscope; STM, scanning tunneling microscope; TEM, transmission electron microscope.

piezoresistive cantilevers in contact mode AFM imaging and manipulation with SEM imaging and FIB etching/deposition[40].

STM/SEM integrated systems have also been developed for simultaneous imaging, manipulation, and measurements[149,150]. A hybrid system that consists of a four-probe STM and an SEM that is coupled to a molecular-beam epitaxy sample preparation chamber was developed for four-point electrical measurements and nanomanipulation of individual atoms to nanowires[150,151].

Both TEMs and SEMs work in high-vacuum conditions. Therefore, water-containing samples cannot be directly observed inside an SEM or TEM[152,153]. Environmental scanning electron microscopes (ESEMs) overcome this limitation and permit the observation of liquid-phase materials, such as biological cells without metal coating and other electrically insulating materials that use a special secondary electron detector[86,154].

The first hybrid AFM/ESEM system was developed for accurate topography measurements and tip–sample interaction observations[52,155]. Although ESEM's imaging resolution is typically limited to a few nanometers, the integrated AFM achieved a resolution better than 0.2 nm in both contact mode AFM imaging and noncontact mode AFM imaging[52]. The nanomanipulation system that was reported in Ref. 90 was constructed inside an ESEM, which consists of two units for manipulation with seven DOFs and one cooling stage for holding samples and sample temperature control. This system performed simultaneous real-time observation and manipulation of biological samples for cell property characterization and surgery[87,91,95,156].

To prepare the TEM samples, a hybrid nanomanipulation system that was integrated with an eight-DOF manipulator and a six-DOF manipulator inside an SEM and a TEM, respectively, was constructed[3,13,153], as shown in Figure 3g. Samples were manipulated and prepared by the SEM manipulator onto the TEM manipulator/holder inside the SEM chamber and subsequently transferred to the TEM for observation and measurement[153].

STATE-OF-THE-ART APPLICATIONS

This section discusses the applications enabled by nanomanipulation inside an SEM, including the characterization of the mechanical and electrical properties of nanoscaled materials and structures, the assembly of nanodevices (for example, biochemical sensors and nanoelectronics and nanophotonics devices), single-cell manipulation and subcellular organelle extraction, and 3D nanoscaled structural reconstruction of organelles.

Manipulation and characterization of nanomaterials

An individual MWNT was EBID-fixed on an AFM cantilever via nanomanipulation to determine the MWNT's Young's modulus[42], as shown in Figure 4a. Mechanical characterization of one-dimensional nanomaterial was also conducted via tensile testing by two AFM cantilevers[50,137]. Using this approach, Zhu et al. conducted in situ tensile testing of a silver nanowire for mechanical characterization of its Young's modulus, yield strength, and ultimate tensile strength[51], as shown in Figure 4b. An InGaAs/GaAs nanospring was stretched for tensile tests using a similar method to determine its stiffness[157,158] (refer to Figure 4c).

Figure 4d shows an example of the characterization of 2D nanomaterials, where 2D nanopaper composed of microfibrillated cellulose was fixed on both ends and driven against a capacitive force sensor probe to perform nanoindentation[159]. Figure 4e shows the indentation of a graphene film using a piezoresistive AFM cantilever. The graphene film was transferred to be suspended on a standard aluminum TEM grid[28,45]. Characteristic force-displacement curves were collected during the indentation process, and the Young's modulus of the graphene films was determined[160]. Figure 4f shows non-destructive measurement using a tuning fork-based end-effector on a batch of suspended
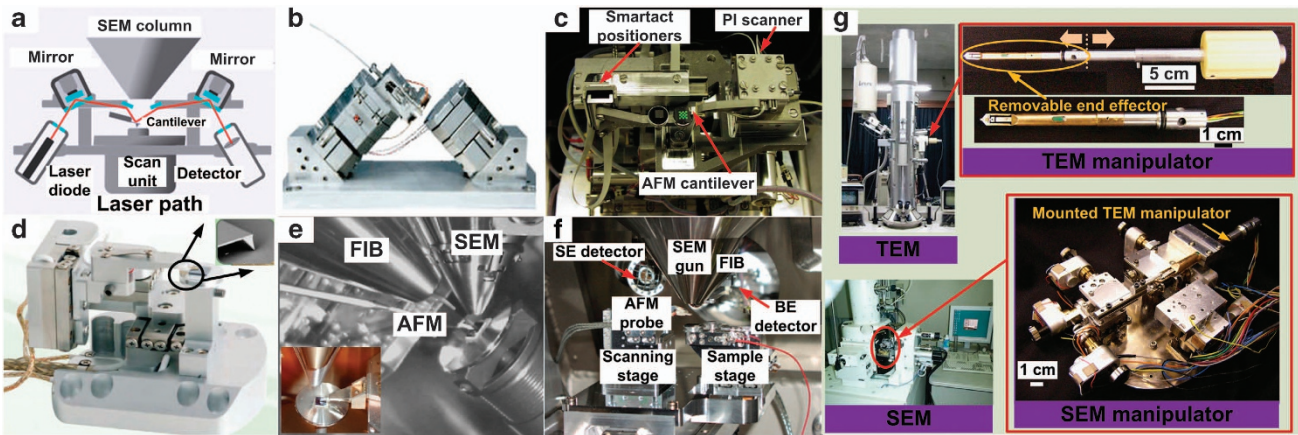
Figure 3 Hybrid system integration inside an SEM. (**a**) A hybrid AFM/SEM system based on laser beam deflection by DME-SPM. (**b**) AttoAFM/ SEM system with a fiber-optic configuration by Attocube Systems AG. (**c**) A hybrid AFM/SEM system using self-sensing piezoresistive cantilevers. Adapted from Ref. 43. (**d**) An AFM system in dynamic mode for SEM integration by Trioptics. (**e**) 3TB4000 AFM/FIB/SEM system from Nanonics Imaging Ltd. (**f**) A hybrid AFM/FIB/SEM system. Adapted from Ref. 40. (**g**) A hybrid SEM and TEM manipulation system. Reprinted with permission from Ref. 13. AFM, atomic force microscope; FIB, focused ion beam; TEM, transmission electron microscope.
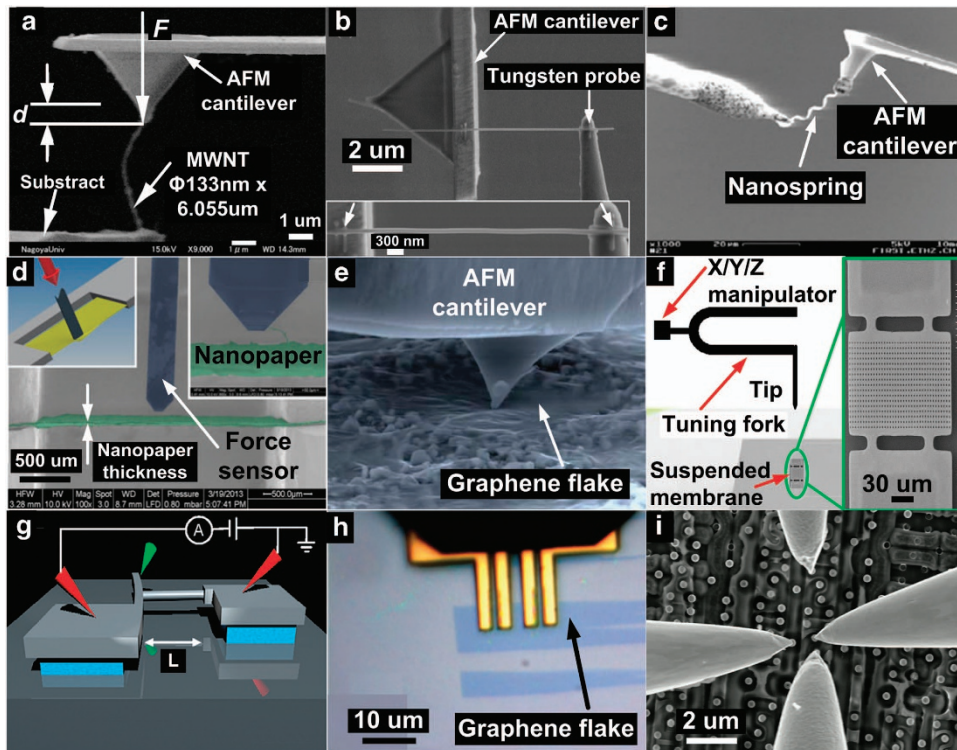

Figure 4 Examples of applications involving mechanical and electrical manipulation and characterization of nanostructures. (**a–c**) Mechanical characterization of MWNTs, nanowires and nanosprings. Adapted from Refs. 42,51,157. (**d–f**) Mechanical characterization of 2D materials of nanopapers, graphene films and suspended InP membranes using nanoindentation and contactless measurements. Adapted from Refs. 148,159,160. (**g–i**) Electrical characterization for nanowires, graphene flakes and single transistors on IC chips. Adapted from Refs. 28,162.

InP membranes to determine their stiffness values[148]. The tuning fork with a QPlus probe was controlled in frequency modulation mode, and the frequency shift was measured to calculate the sample stiffness[161].

Nanomanipulation was also applied to conduct electrical characterization of nanomaterials. Figure 4g illustrates piezoresistivity characterization of a Si nanowire under tensile strain. The Si nanowire's two ends were anchored on a cantilever and an insulated Si pad, respectively. One probe, which was labeled in green in Figure 4g, was used to apply stress to the freestanding cantilever, which generated strain on the Si nanowire. The two probes labeled in red were controlled to form electrical connections to measure the nanowire's electrical resistance changes[162]. For the electrical characterization of graphene, an L-shaped four-point probe was fabricated using FIB and controlled to probe a graphene film[28], as shown in Figure 4h. Nanoprobing
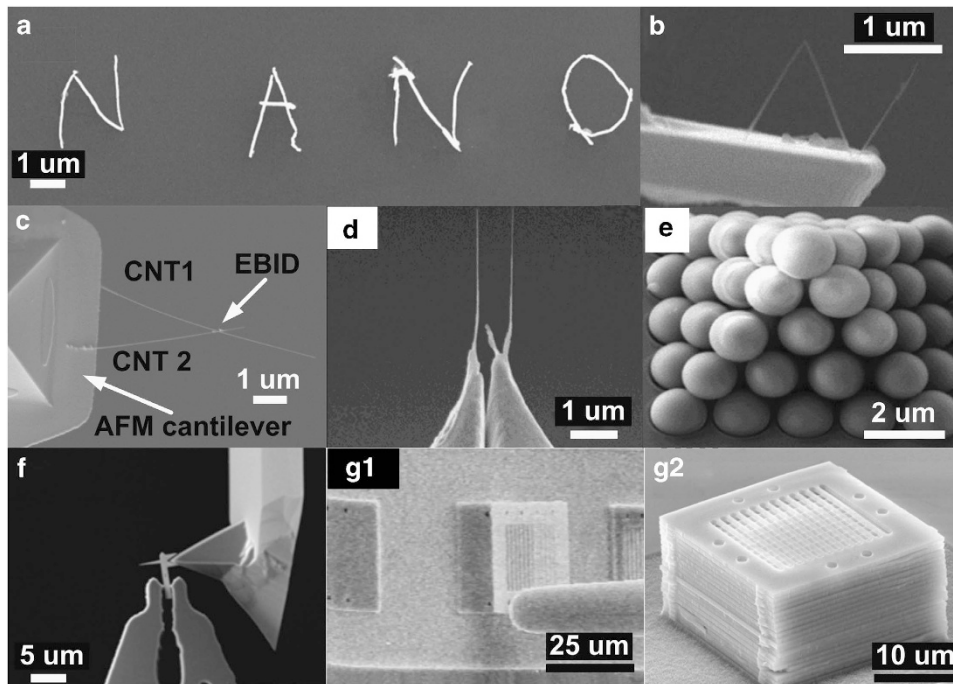
Figure 5 Examples of nano device and nanostructure assembly. (**a**) Nanowires were picked and placed to assemble a nano pattern. Adapted from Ref. 163. (**b**) A MWCNT was formed using a 3D letter with EBID. Adapted from Ref. 13. (**c** and **d**) A thermal sensor and a pair of nanoscaled tweezers were assembled with nanomanipulation. Reprinted with Institute of Physics Publishing (IOP) permission from Ref. 138 and adapted from Ref. 165. (**e**) 3D pyramidal spheres were assembled. Adapted from Ref. 70. (**f**) A nanotool was mounted on an AFM cantilever. Reprinted with IOP permission from Ref. 39. (**g**1 and **g**2) Assembly of photonic plates to form a 3D photonic crystal. Adapted from Ref. 1. EBID, electron-beam-induced deposition; MWCNT, multi-walled CNT.

inside SEM was also employed to attain I–V data of single transistors on IC chips by Kleindiek Nanotechnik (refer to Figure 4i), for identifying faulty locations and understanding failure mechanisms[27].

Assembly of nanodevices

With its precise positioning and manipulation capabilities, nanorobotic manipulation has enabled the assembly of nanostructures and nanodevices. Figure 5a shows that individual gold nanowires were picked and placed by two nanoprobes and subsequently welded and assembled to form the nano pattern 'NANO'[163]. A 3D letter 'N', as shown in Figure 5b, was formed by EBID with oxygen as a precursor for cutting and bending of a MWCNT and nanomanipulation for assembly[13,141,164]. Figure 5c shows a thermal sensor that is composed of two MWCNTs assembled on an AFM cantilever with EBID and nanomanipulation[138]. In Figure 5d, two nanotubes were successively manipulated and assembled to form a pair of nanoscaled tweezers[165]. A DC voltage was applied to open and close the nanotweezers for the pick-and-place of nanoparticles.

A 3D pyramidal structure that consists of stacked silica spheres, as shown in Figure 5e, was assembled via cooperative manipulation using two nanoprobes. A tungsten nanoprobe and a modified piezoresistive AFM cantilever with a spherical adhesion pocket tip were employed to pick and place the silica spheres[70]. In Figure 5f, a custom nanotip was manipulated by a microgripper to approach an AFM cantilever and subsequently soldered and assembled onto the AFM cantilever tip using EBID to construct a high-aspect-ratio AFM cantilever tip for high-resolution imaging[39]. To produce a 3D photonic crystal device (Figure 5g2)[1], a thin plate was separated from a substrate after the connection bridge was broken with a nanoprobe and picked and transferred for assembly, as shown in Figure 5g1.

Nanorobotic manipulation also enabled the assembly of a variety of other NEMS devices[7,22,166,167] for applications in the nanoelectronics and bionanotechnology sectors, as summarized in Table 4.

Cell characterization and manipulation

Standard AFM cantilevers were modified using FIB etching and deposition to produce different types of functional tools, such as a soft buckling nanoneedle[86,90,91], a nano-fork and a nano putter[95,168], as shown in Figures 6a, b and c, respectively. These tools were mounted on a nanomanipulation system in ESEM to perform indentation to determine cell stiffness and viscoelastic properties[87,90]. The nanomanipulation system was also employed to lift and push a cell to measure adhesion forces between the cell and substrate[89,95,156,168]; to measure cell–cell adhesion force[96]; and to electrically characterize intracellular properties[36], as shown in Figures 6d and e. Figure 6f shows the use of a nano-knife for performing cell surgery of a yeast cell[94]. The extraction of DNA from a single-cell nucleus was performed via nanomanipulation under SEM. A nanomanipulation system equipped with a nanospatula as the end-effector was employed to dissect and collect a single-chromatin complex from within a cell nucleus after correlating SEM images and fluorescence microscopy images to determine the target locations to extract[169], as shown in Figures 6g1–g3. Because gene locations within the nucleus are not random, this technique enables high-throughput gene mapping for exploring gene loci associations with nuclear substructures[37].

Automated nanomanipulation

Manual nanomanipulation by a joystick is time-consuming and skill dependent. Over the past decade, progress in automated nanomanipulation tasks has been achieved[49,170]. Table 5 summarizes representative automated nanomanipulation. The majority of automated SEM-based nanomanipulation tasks were

performed with custom instruments using piezoelectric positioners. AFM cantilevers, tungsten probes and MEMS grippers with EBID-assisted soldering techniques are employed for assembly and pick-and-place operation, primarily via SEM-based visual servoing and assisted by force and depth detection. Developing the non-application-specific automated nanomanipulation solutions remains challenging.

Automated pick-and-place of nano objects. In Ref. 112, a MEMS gripper was controlled to automatically pick up a CNT from a

Table 4 Nanoelectromechanical systems (NEMS) constructed by nanomanipulation inside SEM

NEMS		Types	References
Nanotube-based	Nanoactuator	Linear motor	22,31,42
		Linear bearing	42,166
	Nanosensor	Thermal sensor	138
		Mass flow sensor	42
	Nanotool	Nanotweezers	165
		Nanoscissors	42
		SPM probes	112,133
		Field emitters	133,139
Nanowire-based	Nanosensor	Gas sensor	40
	Nanotool	Transistors	32,40,167
Graphene-based	Nanosensor	Oscillator	28

Abbreviations: NEMS, nanoelectromechanical systems.

substrate and place and solder it onto a target structure. Depth-from-focus and depth detection using a piezoelectric touch sensor were employed for coarse and fine alignment to place the microgripper with respect to the CNT in the Z-direction for pick-up[71]. A manipulation strategy using line and two-point contact to adjust adhesion forces was developed to place the CNT onto a target AFM tip to form a CNT-enhanced, high-aspect-ratio AFM tip for scanning deep trenches[112]. For mechanical characterization, individual silicon nanowires were automatically picked up and placed on a MEMS tensile testing device[98,171]. Via visual recognition and vision-based closed-loop control, a nanowire was picked up from the growth substrate and moved for fixation on the MEMS device with EBID. Automated pick-and-place of individual colloidal spheres was realized using two nanoprobes with tailored geometries for cooperative manipulation to form a 3D pyramidal structure via visual servoing and force control[70]. The method did not involve the use of EBID and provided a flexible strategy for 3D nano assembly.

Automated nanoprobing. Nanomanipulation is capable of automated positioning of nanoprobes on nanostructures to perform electrical characterization for fault analysis and quality control. Automated nanoprobing was performed to probe nanostructures on SEM metrology chips, as shown in Figures 7a and b. Algorithms were developed on a GPU to realize real-time SEM image denoising and drift compensation, which enable robust visual tracking and visual servo control for automated nanoprobing[26,27]. Automated four-point probe measurements on single nanowires were also performed for electrical characterization[30], as shown in Figure 7c, where four tungsten nanoprobes were moved
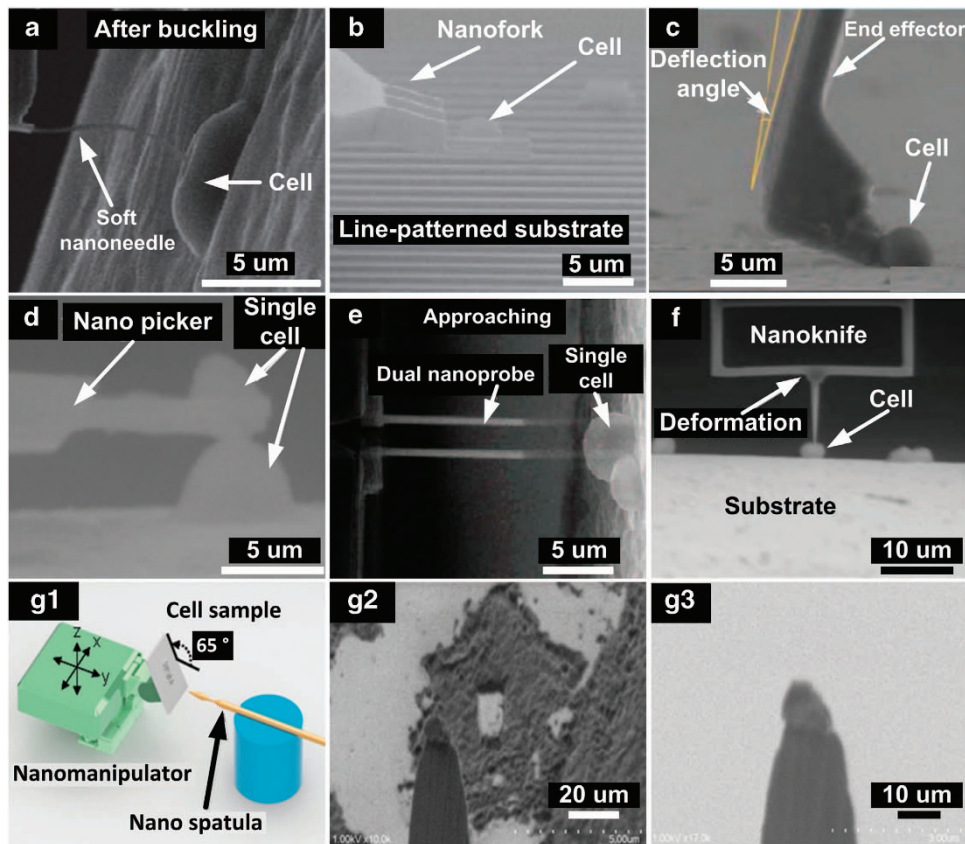

Figure 6 Cell characterization and manipulation inside an ESEM and SEM. (**a**) Cell stiffness measurement. Adapted from Ref. 90. (**b**–**d**) Cell–substrate and cell–cell adhesion force determination. Adapted from Refs 89,95 and reprinted with IOP permission from Ref. 96. (**e**) Intracellular electrical measurement for viability testing. Adapted from Ref. 36. (**f**) Single cell cutting. Reprinted with IOP permission from Ref. 94. (**g**1–**g**3) Chromatin extraction process. Adapted from Ref. 37.

Table 5 Summary of automated nanomanipulation

Task	Nanotool	Feedback	Object size	Success rate	Throughput	References
Pick-and-place of particles	Two end-effectors formed on an AFM cantilever	SEM-based visual servoing; capacitive position sensors; piezoresistive AFM cantilever for contact force detection	1160 nm, 519 nm, 237 nm	100% for 100 particles	112 s per particle	70
Pick-and-place of nanowire	Electrothermal MEMS gripper;	SEM-based visual servoing; piezo bimorph touch sensor for depth sensing	30–150 nm	Not reported	Not reported	71
	Tungsten probes	SEM-based visual servoing	74–113 nm	Not reported	10 min per nanowire	98
Pick-and-place for nanotool assembly	Electrothermal MEMS gripper; FIB modified AFM cantilever	SEM-based visual servoing; optical encoder	3–4 μm long, 150-nm thick	Not reported	Not reported	39
Nanoprobing of nanostructures	Tungsten probes	SEM-based visual servoing	130 nm	Not reported	15.3 s per 2 locations	26
Nanoprobing of nanowires	Tungsten probes	SEM-based visual servoing; vision-based contact-detection	70–100 nm	100% for 50 measurements	20 s per nanowire	30
Membrane indentation	Piezoresistive AFM cantilever	SEM-based visual servoing; piezoresistive indentation force sensing; capacitive position sensors	50-nm thick	Not reported	Not reported	45
Intracellular DNA extraction	Nanospatula	SEM-based visual servoing; strain gauges for position-sensing	100 nm	16%	Not reported	37

Abbreviations: AFM, atomic force microscope; FIB, focused ion beam; SEM, scanning electron microscope.

downward to contact the substrate via a vision-based contact-detection method[72] and subsequently moved upward to a certain height above the substrate. Via visual servo control with a feedforward controller[69,172], the four probes were positioned via closed-loop control to land on their respective target locations along the nanowire at a pre-defined separation distance. The I–V characteristics of the nanowire with regard to different separation distances between the two inner probes are shown in Figure 7d.

SEM-guided, automated AFM manipulation. SEM imaging can be employed to guide the AFM cantilever to localize the regions of interest where AFM imaging or measurement is conducted. A hybrid AFM/FIB/SEM system that employed a piezoresistive cantilever was controlled to realize automated indentation for mechanical characterization of graphene membranes[45]. The piezoresistive cantilever provided force feedback, and a calibration cross-structure by FIB milling was created on its back surface to enable reliable visual tracking of the cantilever. Graphene membranes were automatically picked up and transferred to suspend on a substrate with a grid pattern, as shown in Figure 7e. SEM imaging was utilized to detect the cantilever position and the centers of holes in the pattern and guide the cantilever to perform nanoindentation at the detected centers (Figures 7f and g). Indentation depths and applied forces, as shown in Figure 7h, were measured for determining the Young's modulus values of the graphene membranes.

3D image reconstruction by nanotomography

Ultramicrotomy involves serially cutting and imaging thin slices of a sample under an SEM. It has served an important role in studying the anatomy of cells and tissues in histology and tomography in materials science[173]. In 2004, Denk and Horstmann presented serial block face scanning electron microscopy (SBFSEM)[174], which is a nanomanipulation method for automatically sectioning and 3D reconstructing of tissue structures. The microtome inside an SEM consisted of a moving diamond knife for slicing a sample and an actuator/positioner to advance the specimen after each slice. After each slicing, the remaining block face was imaged[174]. Algorithms for image segmentation and structural reconstruction were developed to generate a 3D tissue nanostructure of biological and other material specimens from the serial images with nanometer resolutions[76].

The development of SBFSEM has enabled advances in neuroscience, in which previous studies have either focused on detailed small volumes or averages over large volumes. SBFSEM bridges the gap by enabling the tracing of neuronal networks and revealing synaptic connections with nanometer resolutions over volumes as large as 1 mm^3 (Ref. 175). The technique is sufficiently fine to resolve morphologies of structures, which can provide clues to their function for a better understanding of certain pathologies. Study tissues that involve long tissue fibers can particularly benefit from SBFSEM. The technique has also been applied in materials science to study the microstructure of engineered materials[176].

DISCOVERIES ENABLED BY SEM-BASED NANOMANIPULATION

Leveraging the technical advances in SEM-based nanomanipulation, many fundamental discoveries have been made, some of which are summarized in Table 6. Mechanical characterization of nanomaterials has significantly benefited from SEM *in situ* nanomanipulation. For instance, nanomanipulation and tensile testing of Ag nanowires of different diameters revealed quantitatively the size and structure effects on the nanowire's mechanical properties (that is, Young's modulus, yield strength, and ultimate tensile strength)[51]. Nanomanipulation was also conducted to perform measurements on silicon nanowires[177] and CNTs[50,137] to
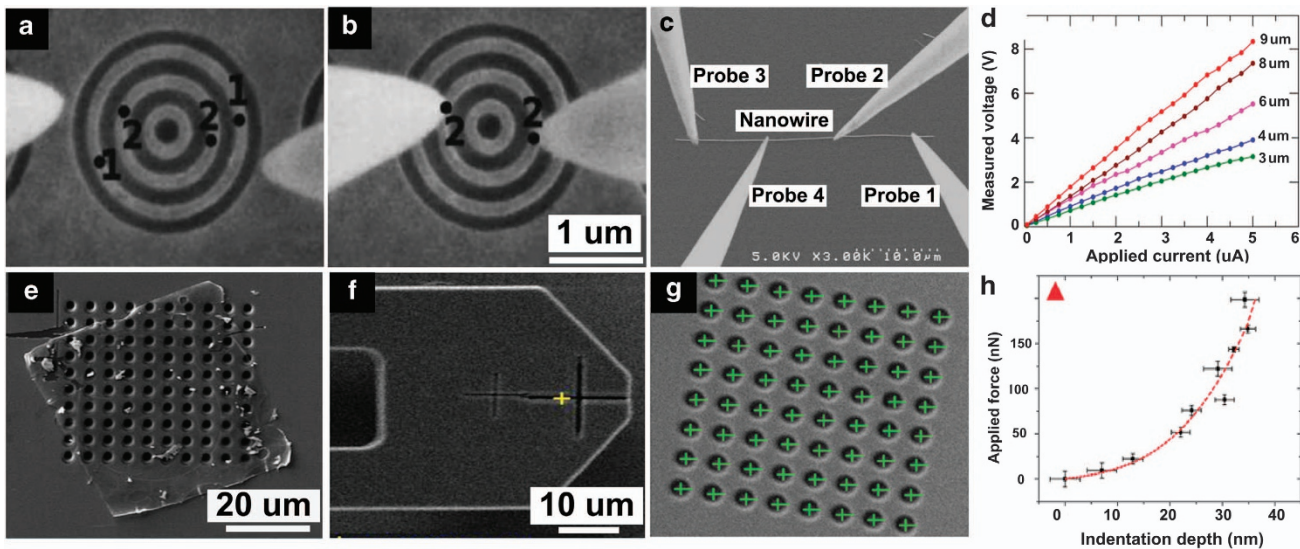
Figure 7 Automated nanomanipulation. (**a** and **b**) Automated nanoprobing. Adapted from Ref. 26. (**c** and **d**) Automated four-point probe measurement on a single nanowire. Adapted from Ref. 30. (**e**–**h**) SEM-guided AFM stiffness measurement of graphene. Adapted from Ref. 45.

Table 6 Examples of discoveries enabled by nanomanipulation inside an SEM

Technique	Field of discovery	Discovery	References
Mechanical testing	Nanomaterials	Young's modulus, yield strength, and ultimate tensile strength of Ag NWs increased as the diameter decreased. Yield strain scaled with surface area, and yielding was caused by dislocation nucleation from surface sources. The pronounced strain hardening was primarily attributed to the presence of internal twin boundaries.	51
	Lithium-ion battery	The delithiated Si nanowire exhibited a significant decrease in the elastic modulus and the ultimate tensile strength owing to the newly formed amorphous Si layers.	178
Electrical nanoprobing	CMOS manufacturing	Strained Si nanowires revealed the positive piezoresistance effect at a low strain level of $< 0.8\%$, whereas an anomalous negative piezoresistance effect and fatigue failure were not observed after several hundred loading cycles for high-strain levels.	162
	Nanomaterials	Large discrete resistance jumps were measured at the random grain boundaries (GBs) in copper nanowires. A metal–insulator transition is revealed in $GdSi_2$ quantum nanowires, whereas a robust metallic state is obtained in wire bundles at low temperatures. The strain effect has served an important role dynamic phase evolution for both phase separation and Mott metal–insulator transition owing to strong electron-lattice coupling.	150,179,180
	Semiconductor	A variation in threshold voltage for each type of cell transistor was normal distribution; marginal failures or degradations that relate to the ultrathin gate oxides, variations in the resistance of the implanted layers in the substrate, and an abnormal passive-voltage-contrast signature were determined.	27
Cellular dissection	Cell biology	Four new gene loci were associated with promyelocytic nuclear bodies, which are tumor-suppression proteins in humans.	37
Cellular characterization	Cell biology	A time effect on yeast cell–cell adhesion force was observed: The force rose to approximately 25 nN with an increase in contact time for the first few minutes and subsequently attained a balance condition with constant force. The stiffness of a single cell decreases with increasing humidity.	93,96
SBFSEM	Neuroscience	Postsynaptic membrane of the predominant synaptic connections were reinforced with use to form a permanent connection, whereas other axons are pruned.	182
	Neuroscience	Synaptic pruning does not proceed normally in the absence of bone morphogenetic proteins, and synapses remain multiply innervated.	183
	Cell biology	A previously unknown ridge-like structure on podocytes was discovered, which changed the understanding of podocyte anatomy.	186

Abbreviations: CMOS, complementary metal-oxide semiconductor; NW, nanowire; SBFSEM, serial block face scanning electron microscopy.

understand how their properties change with size and structure variations. Nanomanipulation and mechanical measurements also shed light on the degradation process of silicon nanowire anodes in lithium-ion batteries[178], contributing to the optimization of battery electrode design for enhanced reliability.

Nanomanipulation and electrical characterization of strained Si nanowires revealed the positive piezoresistive effect at low strain levels and also found carrier mobility enhancement for strained Si-CMOS (silicon-complementary metal-oxide semiconductor) in semiconductor devices[162]. At high-strain levels, the negative piezoresistive effect became apparent, and no fatigue failures occurred after several hundred loading cycles. These findings emphasize the importance of crystallinity and strain for Si nanowires in semiconductor applications[162].

SEM *in situ* electrical characterization of $GdSi_2$ quantum nanowires explained how the electronic transport nature is modified by local atomic defects and interwire coupling in a quantum wire system[179]. The atomic defects produce electron localizations in isolated nanowires, and interwire coupling stabilizes the structure and promotes the metallic states in wire bundles[180]. For IC testing at the transistor level, electrical characterization by nanoprobing inside an SEM was performed to evaluate SRAM cells for failure analyses, which revealed the root causes and failure mechanisms[27] and contributed to the packaging and IC-MEMS integration[181].

Intracellular dissection via nanomanipulation inside an SEM extracted target DNA from a single-cell nucleus to discover gene associations with nuclear bodies[37]. Four new gene loci on chromosomes 11, 17, and 18 that have a significant association with promyelocytic leukemia nuclear bodies, which are tumor-suppression proteins in humans, were discovered. Known gene loci on chromosomes 1 and 6, which are associated with histone locus bodies, were reconfirmed; this finding proves that nano-dissection is a viable method for discovering mechanisms for nuclear event regulation. Nanomanipulation of cellular materials revealed how chemical bonds regulate cell–cell adhesion and its contact-time dependence[96].

SBFSEM was employed to study neuronal circuit development[182]. When new synapses are formed, they are innervated by many axons. During development, the connections carry competing signals, and the axon with the strongest signal remains connected, while the remaining axons withdraw in a process that is referred to as synaptic pruning or synapse elimination. Using SBFSEM, the postsynaptic membrane of an axon that carries the 'winning' signal was reinforced. SBFSEM was also employed to investigate the role of bone morphogenetic proteins (BMPs) in synapse generation and development[183]. In the absence of BMPs, synapse elimination at the calyx of Held in a mouse brain did not occur normally, whereas control mouse neurons undergo normal synapse elimination in the presence of BMPs. Studies have suggested that abnormal synapse elimination may be a risk factor for neurological or psychological diseases[184,185]. The structure of podocytes, which is a type of cell in kidneys that filters blood[186], were also examined using SBFSEM. Three different structures, including the cell body, the primary process, and the foot process, were previously identified. However, the SBFSEM data discovered ridge-like structures on which the foot processes are anchored. These ridge-like structures appear on both the primary process and the cell body; this discovery changes a misunderstanding of podocyte anatomy.

SUMMARY AND OUTLOOK

This paper presented technical advances in the establishment of nanorobotic manipulation laboratories inside SEMs for simultaneous imaging and nanomanipulation. These platforms and nanomanipulation techniques have enabled the *in situ* characterization of nanomaterials, the assembly of nano device

prototypes, and the analysis of subcellular organelles. Despite the significant progress that has been achieved in the past two decades, challenges remain in the realization of 3D nanomanipulation with high precision, robustness, flexibility, and high throughput.

The majority of SEM-based nanomanipulation tasks are manually performed. Although a number of sensing technologies have been developed for integration into nanomanipulation systems, automation remains dependent on SEM imaging as feedback. The low frame rate of SEMs and the high noise, drift, and distortion of real-time SEM imaging hinder the achievement of reliable visual tracking and pose estimation of end-effectors and target objects for high-speed nanomanipulation. Advanced visual tracking methods must be developed to cope with blurred and distorted SEM images. Advanced control schemes that employ integrated information from image-, force-, depth-, and position-sensing modalities are needed for effective decision-making, planning, and manipulation.

During the past decade, efforts have been made in automated nanomanipulation (for example, pick-and-place of CNTs[44] and nanowires for mechanical characterization[98], nanowire field-effect transistor assembly[32]), nanoprobing for electrical characterization of nanowires and transistors[26,30], and SEM-guided AFM manipulation for the transfer and stiffness measurement of graphene membranes[28,45]. Automated nanoprobing has demonstrated higher consistency and at least three times faster operation than manual operation[26], in addition to minimizing the risks of nanotools and sample breakage[30]. Automated pick-and-place of nanowires was completed within 10 min compared with 2 h by teleoperation[98,171]. Although techniques such as visual tracking, depth detection, and the integration of feedback and feedforward control for piezoelectric positioning have been developed for automated nanomanipulation in known environments, system performance may deteriorate in changing environments with uncertain physical parameters and dynamic disturbances.

The application of nanomanipulation has penetrated several disciplines and sectors, such as materials science, semiconductor, cell biology, and neuroscience. Some notable achievements are mechanical and electrical characterization of graphene membranes[28,45], electrical measurement of single transistors[27], 3D transfer of graphene[28,45], assembly of photonic crystal devices[1,187], identification of the size effect on the mechanical properties of nanowires and the strain effect on the piezoresistive properties of nanowires[51,162], discovery of new gene loci associated with promyelocytic nuclear bodies[37], and tracing of neuronal networks and synaptic connections[182,183].

The formation of hybrid systems by integrating other instruments into an SEM has also produced unique capabilities. For instance, STM/SEM integration is capable of manipulating individual atoms; characterizing electrical transport of CNTs, bending, and cutting nanofibers; and fabricating nanowires[151,188]. This integration has also enabled fundamental discoveries of intrinsic structure-transport at the atomic scale[180] and the effect of applied stress on dynamic phase evolution[189]. In addition to STM, nanoscale laboratories inside an SEM have also integrated AFM, FIB, optical microscopes, and multi-tool changers. Further advances in hardware development will produce powerful *in situ* capabilities for manipulation, assembly, and characterization of nanoscales objects and materials to close the gap between current bottom–up and top–down technologies.

With the unique advantages of programmability, automation, and specificity, nanomanipulation inside an SEM will continue to serve as a strong driver of scientific discoveries and further evolve into a more powerful workhorse technology for the nano sciences and nanotechnology industries.

REFERENCES

1 Aoki K, Miyazaki HT, Hirayama H *et al*. Microassembly of semiconductor three-dimensional photonic crystals. *Nature Materials* 2003; **2**: 117–121.

2 Garcia R, Knoll AW, Riedo E. Advanced scanning probe lithography. *Nature Nanotechnology* 2014; **9**: 577–587.

3 Fukuda T, Nakajima M, Ahmad MR *et al*. Micro-and nanomechatronics. *IEEE Industrial Electronics Magazine* 2010; **4**: 13–22.

4 Liu J, Wen J, Zhang Z *et al*. Voyage inside the cell: Microsystems and nanoengineering for intracellular measurement and manipulation. *Microsystems & Nanoengineering* 2015; **1**: 15020.

5 Yost AL, Shahsavari S, Bradwell GM *et al*. Layer-by-layer functionalized nanotube arrays: A versatile microfluidic platform for biodetection. *Microsystems & Nanoengineering* 2015; **1**: 15037.

6 Requicha AAG. Nanorobots, NEMS, and nanoassembly. *Proceedings of the IEEE* 2003; **9**: 1922–1933.

7 Dong L, Nelson BJ. Tutorial—robotics in the small Part II: Nanorobotics. *IEEE Robotics & Automation Magazine* 2007; **14**: 111–121.

8 Fahlbusch S, Mazerolle S, Breguet JM *et al*. Nanomanipulation in a scanning electron microscope. *Journal of Materials Processing Technology* 2005; **167**: 371–382.

9 Esashi M, Kojima A, Ikegami N *et al*. Development of massively parallel electron beam direct write lithography using active-matrix nanocrystalline-silicon electron emitter arrays. *Microsystems & Nanoengineering* 2015; **1**: 15029.

10 Singer JP, Pelligra CI, Kornblum N *et al*. Multiscale patterning of a metallic glass using sacrificial imprint lithography. *Microsystems & Nanoengineering* 2015; **1**: 15040.

11 Parviz BA, Ryan D, Whitesides GM. Using self-assembly for the fabrication of nano-scale electronic and photonic devices. *IEEE Transactions on Advanced Packaging* 2003; **26**: 233–241.

12 Whitesides GM, Grzybowski B. Self-assembly at all scales. *Science* 2002; **295**: 2418–2421.

13 Fukuda T, Nakajima M, Pou L *et al*. Bringing the nanolaboratory inside electron microscopes. *IEEE Nanotechnology Magazine* 2008; **2**: 18–31.

14 Eigler DM, Schweizer EK. Positioning single atoms with a scanning tunnelling microscope. *Nature* 1990; **344**: 524–526.

15 Rubio-Sierra FJ, Heckl WM, Stark RW. Nanomanipulation by atomic force microscopy. *Advanced Engineering Materials* 2005; **7**: 193–196.

16 Russell P, Batchelor D. SEM and AFM: Complementary techniques for surface investigations. *Microscopy and Analysis* 20012001, 9–14.

17 Sitti M. Microscale and nanoscale robotics systems [Grand Challenges of Robotics]. *IEEE Robotics & Automation Magazine* 2007; **14**: 53–60.

18 Tseng AA, Notargiacomo A, Chen TP. Nanofabrication by scanning probe microscope lithography: A review. *Journal of Vacuum Science & Technology B: Microelectronics and Nanometer Structures* 2005; **23**: 877.

19 Hou J, Liu LQ, Wang ZY *et al*. AFM-based robotic nano-hand for stable manipulation at nanoscale. *IEEE Transactions on Automation Science and Engineering* 2013; **10**: 285–295.

20 Zhu Y, Dürr H. The future of electron microscopy. *Physics Today* 2015; **68**: 62.

21 Espinosa HD, Bernal RA, Filleter T. *In situ* TEM electromechanical testing of nanowires and nanotubes. *Small* 2012; **8**: 3233–3252.

22 Dong L, Subramanian A, Nelson BJ. Carbon nanotubes for nanorobotics. *Nano Today* 2007; **2**: 12–21.

23 Hatamura Y, Morishita H. Direct coupling system between nanometer world and human world. IEEE Proceedings of Micro Electro Mechanical Systems, An Investigation of Micro Structures, Sensors, Actuators, Machines and Robots; 11-14 Feb 1990; Napa Valley, CA, USA; 1990: 203–208.

24 Kasaya T, Miyazaki H, Saito S *et al*. Micro object handling under SEM by vision-based automatic control. *SPIE Proceedings* 1998; **3519**: 182–192.

25 Miyazaki H, Sato T. Mechanical assembly of three-dimensional microstructures from fine particles. *Advanced Robotics* 1996; **11**: 169–185.

26 Gong Z, Chen BK, Liu J *et al*. Robotic Probing of Nanostructures inside Scanning Electron Microscopy. *IEEE Transactions on Robotics* 2014; **30**: 758–765.

27 Toh SL, Tan PK, Goh YW *et al*. In-depth electrical analysis to reveal the failure mechanisms with nanoprobing. *IEEE Transactions on Device and Materials Reliability* 2008; **8**: 387–393.

28 Zimmermann S, Garnica Barragan SA, Fatikow S. Nanorobotic processing of graphene: a platform tailored for rapid prototyping of graphene-based devices. *IEEE Nanotechnology Magazine* 2014; **8**: 14–19.

29 Peng LM, Chen Q, Liang XL *et al*. Performing probe experiments in the SEM. *Micron* 2004; **35**: 495–502.

30 Ru C, Zhang Y, Sun Y *et al*. Automated four-point probe measurement of nanowires inside a scanning electron microscope. *IEEE Transactions on Nanotechnology* 2011; **10**: 674–681.

31 Dong L, Nelson BJ, Fukuda T *et al*. Towards nanotube linear servomotors. *IEEE Transactions on Automation Science and Engineering* 2006; **3**: 228–235.

32 Zhang YL, Li J, To S *et al*. Automated nanomanipulation for nanodevice construction. *Nanotechnology* 2012; **23**: 065304.

33 Weck M, Hümmler J, Petersen B. Assembly of hybrid microsystems in a large-chamber scanning electron microscope by use of mechanical grippers. *Proceedings of SPIE* 1997; **3223**: doi:10.1117/12.284484.

34 Xu D, Subramanian A, Dong L *et al*. Shaping nanoelectrodes for high-precision dielectrophoretic assembly of carbon nanotubes. *IEEE Transactions on Nanotechnology* 2009; **8**: 449–456.

35 Shen Y, Fukuda T. State of the art: Micro-nanorobotic manipulation in single cell analysis. *Robotics and Biomimetics* 2014; **1**: 1–13.

36 Ahmad MR, Nakajima M, Kojima M *et al*. Instantaneous and quantitative single cells viability determination using dual nanoprobe inside ESEM. *IEEE Transactions on Nanotechnology* 2012; **11**: 298–306.

37 Chen BK, Anchel D, Gong Z *et al*. Nano-dissection and sequencing of DNA at single sub-nuclear structures. *Small* 2014; **10**: 3267–3274.

38 Sahu B, Taylor CR, Leang KK. Emerging challenges of microactuators for nanoscale positioning, assembly, and manipulation. *Journal of Manufacturing Science and Engineering* 2010; **132**: 030917.

39 Kumar RTR, Hassan SU, Sukas OS *et al*. Nanobits: Customizable scanning probe tips. *Nanotechnology* 2009; **20**: 395703.

40 Fatikow S, Eichhorn V, Bartenwerfer M. Nanomaterials enter the silicon-based cmos era: Nanorobotic technologies for nanoelectronic devices. *IEEE Nanotechnology Magazine* 2012; **6**: 14–18.

41 Zhang YL, Zhang Y, Ru C *et al*. A load-lock-compatible nanomanipulation system for scanning electron microscope. *IEEE/ASME Transactions on Mechatronics* 2013; **18**: 230–237.

42 Fukuda T, Arai F, Dong LX. Assembly of nanodevices with carbon nanotubes through nanorobotic manipulations. *Proceedings of the IEEE* 2003; **91**: 1803–1818.

43 Mick U, Eichhorn V, Wortmann T *et al*. Combined nanorobotic AFM/SEM system as novel toolbox for automated hybrid analysis and manipulation of nanoscale objects. IEEE International Conference on Robotics and Automation (ICRA 2010); 3–7 May 2010; Anchorage, AK, USA; 2010: 4088–4093.

44 Fatikow S, Eichhorn V. Nanohandling automation: Trends and current developments. *Proceedings of the Institution of Mechanical Engineers, Part C Journal of Mechanical Engineering Science* 2008; **222**: 1353–1369.

45 Zimmermann S, Tiemerding T, Li T *et al*. Automated mechanical characterization of 2-D materials using SEM based visual servoing. *International Journal of Optomechatronics* 2013; **7**: 283–295.

46 Sievers T, Fatikow S. Real-time object tracking for the robot-based nanohandling in a scanning electron microscope. *Journal of Micromechatronics* 2006; **3**: 267–284.

47 Yong YK, Moheimani SOR, Kenton BJ *et al*. Invited review article: High-speed flexure-guided nanopositioning: Mechanical design and control issues. *Review of Scientific Instruments* 2012; **83**: 121101.

48 Denisyuk AI, Krasavin AV, Komissarenko FE *et al*. Mechanical, electrostatic, and electromagnetic manipulation of microobjects and nanoobjects in electron microscopes. *Advances In Imaging and Electron Physics* 2014; **186**: 101–140.

49 Fatikow S, Jasper D, Dahmen C *et al*. Robot-based automation on the nanoscale. *Encyclopedia of Nanotechnology* 2012; 2012: 2246–2264.

50 Yu M, Dyer MJ, Skidmore GD *et al*. Three-dimensional manipulation of carbon nanotubes under a scanning electron microscope. *Nanotechnology* 1999; **10**: 244.

51 Zhu Y, Qin Q, Xu F *et al*. Size effects on elasticity, yielding, and fracture of silver nanowires: *In situ* experiments. *Physical Review B* 2012; **85**: 045443.

52 Joachimsthaler I, Heiderhoff R, Balk LJ. A universal scanning-probe-microscope-based hybrid system. *Measurement Science and Technology* 2003; **14**: 87.

53 Romeis S, Paul J, Herre P *et al*. *In situ* deformation and breakage of silica particles inside a SEM. *Procedia Engineering* 2015; **102**: 201–210.

54 Lim SC, Kim KS, Lee IB *et al*. Nanomanipulator-assisted fabrication and characterization of carbon nanotubes inside scanning electron microscope. *Micron* 2005; **36**: 471–476.

55 Fatikow S, Rembold U. *Microsystem Technology And Microbotics*. Springer Science & Business Media; Berlin, Heidelberg, Germany, 2013.

56 Fatikow S, Wich T, Hulsen H *et al*. Microrobot system for automatic nanohandling inside a scanning electron microscope. *IEEE/ASME Transactions on Mechatronics* 2007; **12**: 244–252.

57 Fahlbusch S, Fatikow S. Implementation of self-sensing SPM cantilevers for nanoforce measurement in microbotics. *Ultramicroscopy* 2001; **86**: 181–190.

58 Fuchiwaki O, Aoyama H. Micromanipulation by miniature robots in a SEM vacuum chamber. *Journal of Robotics and Mechatronics* 2002; **14**: 221–226.

59 Fuchiwaki O, Arafuka K, Omura S. Development of 3-DOF Inchworm mechanism for flexible, compact, low-inertia, and omnidirectional precise positioning: Dynamical analysis and improvement of the maximum velocity within no slip of electromagnets. *IEEE/ASME Transactions on Mechatronics* 2012; **17**: 697–708.

60 Kortschack A, Shirinov A, Trüper T, Fatikow S. Development of mobile versatile nanohandling microrobots: Design, driving principles, haptic control. *Robotica* 2005; **23**: 419–434.

61 Chi ZQ, Xu QS. Recent advances in the control of piezoelectric actuators. *International Journal of Advanced Robotic Systems* 2014; 2014: doi: 10.5772/59099.

62 Rakotondrabe M, Ivan IA, Khadraoui S *et al*. Simultaneous displacement/force self-sensing in piezoelectric actuators and applications to robust control. *IEEE/ASME Transactions on Mechatronics* 2015; **20**: 519–531.

63 Yong YK, Fleming AJ, Moheimani SO. A novel piezoelectric strain sensor for simultaneous damping and tracking control of a high-speed nanopositioner. *IEEE/ASME Transactions on Mechatronics* 2013; **18**: 1113–1121.

64 Zhou C, Gong Z, Chen B *et al*. A closed-loop controlled nanomanipulation system for probing nanostructures inside scanning electron microscopes. *IEEE/ASME Transactions on Mechatronics* 2016; **21**: 1233–1241.

65 Fleming AJ. A review of nanometer resolution position sensors: Operation and performance. *Sensors and Actuators A*: *Physical* 2013; **190**: 106–126.

66 Fatikow S, Eichhorn V, Stolle C *et al*. Development and control of a versatile nanohandling robot cell. *Mechatronics* 2008; **18**: 370–380.

67 Jahnisch M, Fatikow S. 3-D vision feedback for nanohandling monitoring in a scanning electron microscope. *International Journal of Optomechatronics* 2007; **1**: 4–26.

68 Wich T, Stolle C, Mikczinski M *et al*. Approach for the 3D-alignment in micro- and nano-scale assembly processes. In: Ratchev S, editor. *Precision Assembly Technologies and Systems*, Volume 315. IFIP Advances in Information and Communication Technology. Springer; Berlin, Heidelberg, Germany; 2010: 167–173.

69 Ru C, Zhang Y, Huang H *et al*. An improved visual tracking method in scanning electron microscope. *Microscopy and Microanalysis: The Official Journal of Microscopy Society of America, Microbeam Analysis Society, Microscopical Society of Canada* 2012; **18**: 612–620.

70 Zimmermann S, Tiemerding T, Fatikow S. Automated robotic manipulation of individual colloidal particles using vision-based control. *IEEE/ASME Transactions on Mechatronics* 2015; **20**: 2031–2038.

71 Eichhorn V, Fatikow S, Wich T *et al*. Depth-detection methods for microgripper based CNT manipulation in a scanning electron microscope. *Journal of Micro-Nano Mechatronics* 2008; **4**: 27–36.

72 Ru C, To S. Contact detection for nanomanipulation in a scanning electron microscope. *Ultramicroscopy* 2012; **118**: 61–66.

73 Kasaya T, Miyazaki HT, Saito S *et al*. Image-based autonomous micromanipulation system for arrangement of spheres in a scanning electron microscope. *Review of Scientific Instruments* 2004; **75**: 2033.

74 Cvetanovic A, Cvetanovic A, Deutschinger A *et al*. Design of a novel visual and control system for the prevention of the collision during the micro handling in a SEM chamber. *Microelectronic Engineering* 2010; **87**: 139–143.

75 Fatikow S, Wich T, Sievers T *et al*. Automatic nanohandling station inside a scanning electron microscope. *Proceedings of the Institution of Mechanical Engineers, Part B: Journal of Engineering Manufacture* 2008; **222**: 117–128.

76 Ribeiro E, Shah M. Computer vision for nanoscale imaging. *Machine Vision and Applications* 2006; **17**: 147–162.

77 Yong Z, Tzu-Hsuan C. A review of microelectromechanical systems for nanoscale mechanical characterization. *Journal of Micromechanics and Microengineering* 2015; **25**: 093001.

78 Fahlbusch S. Force feedback for nanohandling. In: Fatikow S, editor. Automated Nanohandling by Microrobots, Springer Series in Advanced Manufacturing. Springer; London, UK; 2008; 167–202.

79 Liang Q, Zhang D, Coppola G *et al*. Multi-dimensional MEMS/micro sensor for force and moment sensing: A review. *IEEE Sensors Journal* 2014; **14**: 2643–2657.

80 Kim K, Sun Y, Voyles RM *et al*. Calibration of multi-axis MEMS force sensors using the shape-from-motion method. *IEEE Sensors Journal* 2007; **7**: 344–351.

81 Sun Y, Nelson BJ. MEMS capacitive force sensors for cellular and flight biomechanics. *Biomedical Materials* 2007; **2**: S16.

82 Sun Y, Nelson BJ, Potasek DP *et al*. A bulk microfabricated multi-axis capacitive cellular force sensor using transverse comb drives. *Journal of Micromechanics and Microengineering* 2002; **12**: 832.

83 Beyeler F, Muntwyler S, Nelson BJ. A six-axis MEMS force-torque sensor with micro-newton and nano-newtonmeter resolution. *Journal of Microelectromechanical Systems* 2009; **18**: 433–441.

84 Domanski K, Janus P, Grabiec P *et al*. Design, fabrication and characterization of force sensors for nanorobot. *Microelectronic Engineering* 2005; **78-79**: 171–177.

85 Chawda V, O'Malley MK. Vision-based force sensing for nanomanipulation. *IEEE/ASME Transactions on Mechatronics* 2011; **16**: 1177–1183.

86 Ahmad MR, Nakajima M, Kojima S *et al*. The effects of cell sizes, environmental conditions, and growth phases on the strength of individual W303 yeast cells inside ESEM. *IEEE Transactions on Nanobioscience* 2008; **7**: 185–193.

87 Ahmad MR, Nakajima M, Kojima S *et al*. Nanoindentation methods to measure viscoelastic properties of single cells using sharp, flat, and buckling tips inside ESEM. *IEEE Transactions on Nanobioscience* 2010; **9**: 12–23.

88 Greminger MA, Nelson BJ. Vision-based force measurement. *IEEE Transactions on Pattern Analysis and Machine Intelligence* 2004; **26**: 290–298.

89 Shen Y, Ahmad MR, Nakajima M *et al*. Evaluation of the single yeast cell's adhesion to ITO substrates with various surface energies via ESEM nanorobotic manipulation system. *IEEE Transactions on Nanobioscience* 2011; **10**: 217–224.

90 Ahmad MR, Nakajima M, Kojima S *et al*. In situ single cell mechanics characterization of yeast cells using nanoneedles inside environmental SEM. *IEEE Transactions on Nanotechnology* 2008; **7**: 607–616.

91 Ahmad MR, Nakajima M, Kojima S *et al*. Buckling nanoneedle for characterizing single cells mechanics inside environmental SEM. *IEEE Transactions on Nanotechnology* 2011; **10**: 226–236.

92 Liu H, Wen J, Xiao Y *et al*. In situ mechanical characterization of the cell nucleus by atomic force microscopy. *ACS Nano* 2014; **8**: 3821–3828.

93 Shen Y, Nakajima M, Yang Z *et al*. Single cell stiffness measurement at various humidity conditions by nanomanipulation of a nano-needle. *Nanotechnology* 2013; **24**: 145703.

94 Shen Y, Nakajima M, Yang Z *et al*. Design and characterization of nanoknife with buffering beam for in situ single-cell cutting. *Nanotechnology* 2011; **22**: 305701.

95 Ahmad MR, Nakajima M, Kojima M *et al*. Nanofork for single cells adhesion measurement via ESEM-nanomanipulator system. *IEEE Transactions on Nanobioscience* 2012; **11**: 70–78.

96 Shen Y, Nakajima M, Kojima S *et al*. Study of the time effect on the strength of cell-cell adhesion force by a novel nano-picker. *Biochemical and Biophysical Research Communications* 2011; **409**: 160–165.

97 Wei X, Chen Q, Peng L *et al*. In situ measurements on individual thin carbon nanotubes using nanomanipulators inside a scanning electron microscope. *Ultramicroscopy* 2010; **110**: 182–189.

98 Ye X, Zhang Y, Ru C *et al*. Automated pick-place of silicon nanowires. *IEEE Transactions on Automation Science and Engineering* 2013; **10**: 554–561.

99 Qing C, Sheng W, Lian-Mao P. Establishing Ohmic contacts for in situ current-voltage characteristic measurements on a carbon nanotube inside the scanning electron microscope. *Nanotechnology* 2006; **17**: 1087.

100 Bøggild P. 3D Biomanipulation Using Microgrippers. Micro and Nano Techniques for the Handling of Biological Samples. CRC Press; Boca Raton, FL, USA; 2011: 141.

101 Kim K, Liu X, Zhang Y *et al*. Elastic and viscoelastic characterization of microcapsules for drug delivery using a force-feedback MEMS microgripper. *Biomedical Microdevices* 2009; **11**: 421–427.

102 Kim K, Liu X, Zhang Y *et al*. Nanonewton force-controlled manipulation of biological cells using a monolithic MEMS microgripper with two-axis force feedback. *Journal of Micromechanics and Microengineering* 2008; **18**: 055013.

103 Andersen KN, Petersen DH, Carlson K *et al*. Multimodal electrothermal silicon microgrippers for nanotube manipulation. *IEEE Transactions on Nanotechnology* 2009; **8**: 76–85.

104 De Lit P, Agnus J, Clévy C *et al*. A four-degree-of-freedom microprehensile microrobot on chip. *Assembly Automation* 2004; **24**: 33–42.

105 Perez R, Agnus J, Clevy C *et al*. Modeling, fabrication, and validation of a high-performance 2-DoF piezoactuator for micromanipulation. *IEEE/ASEM Transactions on Mechatronics* 2005; **10**: 161–171.

106 Zhang Y, Chen BK, Liu X *et al*. Autonomous robotic pick-and-place of microobjects. *IEEE Transactions on Robotics* 2010; **26**: 200–207.

107 Chen BK, Zhang Y, Perovic DD *et al*. MEMS microgrippers with thin gripping tips. *Journal of Micromechanics and Microengineering* 2011; **21**: 105004.

108 Chen BK, Zhang Y, Sun Y. Active release of microobjects using a MEMS microgripper to overcome adhesion forces. *Journal of Microelectromechanical Systems* 2009; **18**: 652–659.

109 Mølhave K, Wich T, Kortschack A *et al*. Pick-and-place nanomanipulation using microfabricated grippers. *Nanotechnology* 2006; **17**: 2434.

110 Mølhave K, Hansen TM, Madsen DN *et al.* Towards pick-and-place assembly of nanostructures. *Journal of Nanoscience and Nanotechnology* 2004; **4**: 279–282.

111 Andersen KN, Carlson K, Petersen DH *et al.* Electrothermal microgrippers for pick-and-place operations. *Microelectronic Engineering* 2008; **85**: 1128–1130.

112 Carlson K, Andersen KN, Eichhorn V *et al.* A carbon nanofibre scanning probe assembled using an electrothermal microgripper. *Nanotechnology* 2007; **18**: 345501.

113 Cédric C, Arnaud H, Joël A *et al.* A micromanipulation cell including a tool changer. *Journal of Micromechanics and Microengineering* 2005; **15**: S292.

114 Clévy C, Hubert A, Chaillet N. Flexible micro-assembly system equipped with an automated tool changer. *Journal of Micro-Nano Mechatronics* 2008; **4**: 59–72.

115 Briston KJ, Cullis AG, Inkson BJ. Fabrication of a novel SEM microgripper by electrochemical and FIB techniques. *Journal of Micromechanics and Microengineering* 2010; **20**: 015028.

116 Liu X, Kim K, Zhang Y *et al.* Nanonewton force sensing and control in microrobotic cell manipulation. *International Journal of Robotics Research* 2009; **28**: 1065–1076.

117 Becker M, Bartenwerfer M, Eichhorn V *et al.* Cantilever based connector platform for exchangeable and customizable scanning probe tips. *Procedia Engineering* 2012; **47**: 220–223.

118 Qin Y, Tian Y, Zhang D *et al.* A novel direct inverse modeling approach for hysteresis compensation of piezoelectric actuator in feedforward applications. *IEEE/ASME Transactions on Mechatronics* 2013; **18**: 981–989.

119 Gu GY, Yang MJ, Zhu LM. Real-time inverse hysteresis compensation of piezoelectric actuators with a modified Prandtl-Ishlinskii model. *The Review of Scientific Instruments* 2012; **83**: 065106.

120 Ru C, Sun L. Hysteresis and creep compensation for piezoelectric actuator in open-loop operation. *Sensors and Actuators A: Physical* 2005; **122**: 124–130.

121 Schitter G, Thurner PJ, Hansma PK. Design and input-shaping control of a novel scanner for high-speed atomic force microscopy. *Mechatronics* 2008; **18**: 282–288.

122 Rakotondrabe M, Clevy C, Lutz P. Complete open loop control of hysteretic, creeped, and oscillating piezoelectric cantilevers. *IEEE Transactions on Automation Science and Engineering* 2010; **7**: 440–450.

123 Bolopion A, Regnier S. A review of haptic feedback teleoperation systems for micromanipulation and microassembly. *IEEE Transactions on Automation Science and Engineering* 2013; **10**: 496–502.

124 Bolopion A, Dahmen C, Stolle C *et al.* Vision-based haptic feedback for remote micromanipulation in-SEM environment. *International Journal of Optomechatronics* 2012; **6**: 236–252.

125 Li D, Rong W, Song J *et al.* SEM image-based 3-D nanomanipulation information extraction and closed-loop probe control. *IEEE Transactions on Nanotechnology* 2014; **13**: 1194–1203.

126 Sharma G, Mavroidis C, Ferreira A. Virtual reality and haptics in nano-and bio-nanotechnology. *Handbook of Theoretical and Computational Nanotechnology* 2005; **10**: 1–33.

127 Ouarti N, Sauvet B, Régnier S. High quality real-time video with scanning electron microscope using total variation algorithm on a graphics processing unit. *International Journal of Optomechatronics* 2012; **6**: 163–178.

128 Kratochvil BE, Dong L, Nelson BJ. Real-time rigid-body visual tracking in a scanning electron microscope. *The International Journal of Robotics Research* 2009; **28**: 498–511.

129 Jasper D, Fatikow S. Line scan-based high-speed position tracking inside the SEM. *International Journal of Optomechatronics* 2010; **4**: 115–135.

130 Dahmen C, Tiemerding T. Fast and robust position determination in the scanning electron microscope. *Proceedings of Australasian Conference on Robotics and Automation 2013.* 2–4 December 2013; Sydney, Australia; 2013.

131 Drummond T, Cipolla R. Real-time visual tracking of complex structures. *IEEE Transactions on Pattern Analysis and Machine Intelligence* 2002; **24**: 932–946.

132 Pressigout M, Marchand E. Real-time hybrid tracking using edge and texture information. *The International Journal of Robotics Research* 2007; **26**: 689–713.

133 Dong L, Arai F, Fukuda T. Electron-beam-induced deposition with carbon nanotube emitters. *Applied Physics Letters* 2002; **81**: 1919–1921.

134 Dong L, Arai F, Fukuda T. Nanoassembly of carbon nanotubes through mechanochemical nanorobotic manipulations. *Japanese Journal of Applied Physics* 2003; **42**: 295.

135 Koops HW, Kretz J, Rudolph M *et al.* Characterization and application of materials grown by electron-beam-induced deposition. *Japanese Journal of Applied Physics* 1994; **33**: 7099.

136 Utke I, Moshkalev S, Russell P. Nanofabrication Using Focused Ion and Electron Beams: Principles and Applications. Oxford University Press; Oxford, UK, 2012.

137 Yu MF, Lourie O, Dyer MJ *et al.* Strength and breaking mechanism of multiwalled carbon nanotubes under tensile load. *Science* 2000; **287**: 637–640.

138 Yang Z, Wang P, Shen Y *et al.* Dual-MWCNT probe thermal sensor assembly and evaluation based on nanorobotic manipulation inside a field-emission-scanning electron microscope. *International Journal of Advanced Robotic Systems* 2015; **12**: 21.

139 Yang Z, Nakajima M, Saito Y *et al.* Isolated high-purity platinum nanowire growth via field emission from a multi-walled carbon nanotube. *Applied Physics Express* 2011; **4**: 035001.

140 Dong L, Arai F, Fukuda T. Destructive constructions of nanostructures with carbon nanotubes through nanorobotic manipulation. *IEEE/ASME Transactions on Mechatronics* 2004; **9**: 350–357.

141 Liu P, Arai F, Fukuda T. Cutting of carbon nanotubes assisted with oxygen gas inside a scanning electron microscope. *Applied Physics Letters* 2006; **89**: 113104-04-3.

142 Fukuda T, Nakajima M, Liu P *et al.* Nanofabrication, nanoinstrumentation and nanoassembly by nanorobotic manipulation. *The International Journal of Robotics Research* 2009; **28**: 537–547.

143 Yang Z, Nakajima M, Ode Y *et al.* Tungsten/platinum hybrid nanowire growth via field emission using nanorobotic manipulation. *Journal of Nanotechnology* 2011; **2011**: 1–8.

144 Kaminskyj SG, Dahms TE. High spatial resolution surface imaging and analysis of fungal cells using SEM and AFM. *Micron* 2008; **39**: 349–361.

145 Wolfgang H-G, Dorothee H, Klaus-Peter J *et al.* Current limitations of SEM and AFM metrology for the characterization of 3D nanostructures. *Measurement Science and Technology* 2011; **22**: 094003.

146 Kimitake F, Daisuke S, Hideki K. Development of a Versatile Atomic Force Microscope within a Scanning Electron Microscope. *Japanese Journal of Applied Physics* 2000; **39**: 3747.

147 Stahl U, Yuan CW, de Lozanne AL *et al.* Atomic force microscope using piezo-resistive cantilevers and combined with a scanning electron microscope. *Applied Physics Letters* 1994; **65**: 2878v.

148 Abrahamians JO, Sauvet B, Polesel-Maris J *et al.* A nanorobotic system for *in situ* stiffness measurements on membranes. *IEEE Transactions on Robotics* 2014; **30**: 119–124.

149 Kaneko A, Homma Y, Hibino H *et al.* Ultrahigh vacuum scanning electron microscope system combined with wide-movable scanning tunneling microscope. *Review of Scientific Instruments* 2005; **76**: 083709.

150 Kim T-H, Wang Z, Wendelken JF *et al.* A cryogenic Quadraprobe scanning tunneling microscope system with fabrication capability for nanotransport research. *Review of Scientific Instruments* 2007; **78**: 123701.

151 Qin S, Kim T-H, Wang Z *et al.* Nanomanipulation and nanofabrication with multi-probe scanning tunneling microscope: From individual atoms to nanowires. *Review of Scientific Instruments* 2012; **83**: 063704.

152 Koster AJ, Klumperman J. Electron microscopy in cell biology: integrating structure and function. *Nature Reviews Molecular Cell Biology* 2003; **4**: SS6–SS9.

153 Nakajima M, Arai F, Fukuda T. *In situ* measurement of Young's modulus of carbon nanotubes inside a TEM through a hybrid nanorobotic manipulation system. *IEEE Transactions On Nanotechnology* 2006; **5**: 243–248.

154 Castillo J, Dimaki M, Svendsen WE. Manipulation of biological samples using micro and nano techniques. *Integrative Biology* 2009; **1**: 30–42.

155 Ch T, Heiderhoff R, Balk LJ. Acoustic near-field conditions in an ESEM/AFM hybrid system. *Journal of Physics: Conference Series* 2007; **61**: 1180.

156 Shen Y, Nakajima M, Zhang Z *et al.* Dynamic force characterization microscopy based on Integrated Nanorobotic AFM and SEM System for Detachment Process Study. *IEEE/ASME Transactions on Mechatronics* 2015; **20**: 3009–3017.

157 Bell DJ, Dong L, Nelson BJ *et al.* Fabrication and characterization of three-dimensional InGaAs/GaAs nanosprings. *Nano Letters* 2006; **6**: 725–729.

158 Bell DJ, Sun Y, Zhang L *et al.* Three-dimensional nanosprings for electromechanical sensors. *Sensors and Actuators A: Physical* 2006; **130–131**: 54–61.

159 Mikczinski MR, Josefsson G, Chinga-Carrasco G *et al.* Nanorobotic testing to assess the stiffness properties of nanopaper. *IEEE Transactions on Robotics* 2014; **30**: 115–119.

160 Zimmermann S, Eichhorn V, Fatikow S. Nanorobotic transfer and characterization of graphene flakes. IEEE/RSJ International Conference on Intelligent Robots and Systems (IROS 2012); 7–12 Oct 2012; Vilamoura, Portugal; 2012: 640–645.

161 Castellanos-Gomez A, Agraït N, Rubio-Bollinger G. Dynamics of quartz tuning fork force sensors used in scanning probe microscopy. *Nanotechnology* 2009; **20**: 215502.

162 Lugstein A, Steinmair M, Steiger A *et al.* Anomalous piezoresistance effect in ultrastrained silicon nanowires. *Nano Letters* 2010; **10**: 3204–3208.

163 Peng Y, Cullis T, Inkson B. Bottom-up nanoconstruction by the welding of individual metallic nanoobjects using nanoscale solder. *Nano Letters* 2009; **9**: 91–96.

164 Liu P, Kantola K, Fukuda T *et al.* Nanoassembly of nanostructures by cutting, bending and soldering of carbon nanotubes with electron beam. *Journal of Nanoscience and Nanotechnology* 2009; **9**: 3040–3045.

165 Seiji A, Yoshikazu N. Manipulation of nanomaterial by carbon nanotube nanotweezers in scanning probe microscope. *Japanese Journal of Applied Physics* 2002; **41**: 4242.

166 Subramanian A, Dong LX, Tharian J *et al.* Batch fabrication of carbon nanotube bearings. *Nanotechnology* 2007; **18**: 075703.

167 Li J, Zhang Y, To S *et al*. Effect of nanowire number, diameter, and doping density on nano-FET biosensor sensitivity. *ACS Nano* 2011; **5**: 6661–6668.

168 Shen Y, Nakajima M, Kojima S *et al*. Single cell adhesion force measurement for cell viability identification using an AFM cantilever-based micro putter. *Measurement Science and Technology* 2011; **22**: 115802.

169 Gong Z, Chen BK, Liu J *et al*. Fluorescence and SEM correlative microscopy for nanomanipulation of subcellular structures. *Light: Science & Applications* 2014; **3**: e224.

170 Fatikow S, Eichhorn V, Krohs F *et al*. Development of automated microrobot-based nanohandling stations for nanocharacterization. *Microsystem Technologies* 2008; **14**: 463–474.

171 Zhang Y, Liu XY, Ru CH *et al*. Piezoresistivity Characterization of Synthetic Silicon Nanowires Using a MEMS Device. *Journal of Microelectromechanical Systems* 2011; **20**: 959–967.

172 Ru C, Sun L. Improving positioning accuracy of piezoelectric actuators by feedforward hysteresis compensation based on a new mathematical model. *Review of Scientific Instruments* 2005; **76**: 095111.

173 Möbus G, Inkson BJ. Nanoscale tomography in materials science. *Materials Today* 2007; **10**: 18–25.

174 Denk W, Horstmann H. Serial block-face scanning electron microscopy to reconstruct three-dimensional tissue nanostructure. *PLoS Biology* 2004; **2**: e329.

175 Andres B, Koethe U, Kroeger T *et al*. 3D segmentation of SBFSEM images of neuropil by a graphical model over supervoxel boundaries. *Medical Image Analysis* 2012; **16**: 796–805.

176 Zankel A, Kraus B, Poelt P *et al*. Ultramicrotomy in the ESEM, a versatile method for materials and life sciences. *Journal of Microscopy* 2009; **233**: 140–148.

177 Zhu Y, Xu F, Qin Q *et al*. Mechanical properties of vapor-liquid-solid synthesized silicon nanowires. *Nano Letters* 2009; **9**: 3934–3939.

178 Boles ST, Sedlmayr A, Kraft O *et al*. *In situ* cycling and mechanical testing of silicon nanowire anodes for lithium-ion battery applications. *Applied Physics Letters* 2012; **100**: 243901.

179 Kim TH, Zhang XG, Nicholson DM *et al*. Large discrete resistance jump at grain boundary in copper nanowire. *Nano Letters* 2010; **10**: 3096–3100.

180 Qin S, Kim TH, Zhang Y *et al*. Correlating electronic transport to atomic structures in self-assembled quantum wires. *Nano Letters* 2012; **12**: 938–942.

181 Fischer AC, Forsberg F, Lapisa M *et al*. Integrating MEMS and ICs. *Microsystems & Nanoengineering* 2015; **1**: 15005.

182 Holcomb PS, Hoffpauir BK, Hoyson MC *et al*. Synaptic inputs compete during rapid formation of the calyx of Held: A new model system for neural development. *The Journal of Neuroscience* 2013; **33**: 12954–12969.

183 Xiao L, Michalski N, Kronander E *et al*. BMP signaling specifies the development of a large and fast CNS synapse. *Nature Neuroscience* 2013; **16**: 856–864.

184 Stevens B, Allen NJ, Vazquez LE *et al*. The classical complement cascade mediates CNS synapse elimination. *Cell* 2007; **131**: 1164–1178.

185 Boksa P. Abnormal synaptic pruning in schizophrenia: Urban myth or reality? *Journal of Psychiatry & Neuroscience* 2012; **37**: 75–77.

186 Ichimura K, Miyazaki N, Sadayama S *et al*. Three-dimensional architecture of podocytes revealed by block-face scanning electron microscopy. *Scientific Reports* 2015; **5**: 8993.

187 Miyazaki HT, Miyazaki H, Ohtaka K *et al*. Photonic band in two-dimensional lattices of micrometer-sized spheres mechanically arranged under a scanning electron microscope. *Journal of Applied Physics* 2000; **87**: 7152–7158.

188 Tae-Hwan K, John FW, An-Ping L *et al*. Probing electrical transport in individual carbon nanotubes and junctions. *Nanotechnology* 2008; **19**: 485201.

189 Kim TH, Angst M, Hu B *et al*. Imaging and manipulation of the competing electronic phases near the Mott metal-insulator transition. *Proceedings of the National Academy of Sciences of the United States of America* 2010; **107**: 5272–5275.